

# Optical dipole mirror for cold atoms based on a metallic diffraction grating

Tomasz Kawalec,<sup>1,\*</sup> Dobrosława Bartoszek-Bober,<sup>1,2</sup> Roman Panaś,<sup>1</sup>  
Jacek Fiutowski,<sup>3</sup> Aleksandra Pławecka,<sup>1</sup> and Horst-Günter Rubahn<sup>3</sup>

<sup>1</sup>*Marian Smoluchowski Institute of Physics, Jagiellonian University, Reymonta 4, 30-059 Krakow, Poland*

<sup>2</sup>*Institute of Physics, Faculty of Physics, Astronomy and Informatics,  
Nicolaus Copernicus University, Grudziadzka 5, 87-100 Torun, Poland*

<sup>3</sup>*Mads Clausen Institute, NanoSyd, University of Southern Denmark, Alsion 2, DK-6400 Sønderborg, Denmark*

compiled: April 14, 2014

We report on the realization of a plasmonic dipole mirror for cold atoms based on a metallic grating coupler. A cloud of atoms is reflected by the repulsive potential generated by surface plasmon polaritons excited on a reflection gold grating by a 780 nm laser beam. Experimentally and numerically determined mirror efficiencies are close to 100 %. The intensity of SPPs above a real grating coupler and the atomic trajectories as well as the momentum dispersion of the atom cloud being reflected are computed. A suggestion is given on how the plasmonic mirror might serve as an optical atom chip.

*OCIS codes:* (020.3320) Laser cooling; (240.6680) Surface plasmons; (230.1950) Diffraction gratings; (230.4000) Microstructure fabrication;  
<http://dx.doi.org/10.1364/XX.99.099999>

Surface plasmon polaritons (SPPs) are electromagnetic excitations resulting from the coupling between an electromagnetic field and collective oscillations of the conduction electrons in a metal [1]. They are associated with an evanescent light wave on both sides of a dielectric-metal interface. In recent years, surface plasmon polaritons have received increasing interest due to their peculiar properties and broad range of applications in optics, spectroscopy, data storage, solar cells, sensors, medical science, etc. [2].

The rapidly growing field of plasmonics starts also to be attractive for manipulation and control of matter at micro, nano and atomic scales, especially when it comes to the investigation of ultracold quantum gases and precise positioning of atoms. In typical experiments, clouds of atoms can be cooled down to nanokelvin temperatures and trapped by means of magnetic and optical potentials. However, the spatial resolution of typical optical traps is limited by diffraction. Plasmonic potentials, which can be structured with subwavelength resolution, offer a promising nanoscale alternative for ultracold atom manipulation, trapping or guiding.

The main component of surface based optical tools for cold and ultracold atoms is an optical dipole mirror. Typical mirrors use a repulsive force associated with a high intensity gradient of the evanescent field excited

in the vicinity of a dielectric prism (see e.g. [3–6] and references therein) or a dielectric planar waveguide [7]. For low saturation, the dispersive part of the atom-field interaction might be described in terms of a dipole potential  $U_{dip}$  of the form

$$U_{dip}(\vec{r}) = \frac{\lambda^3}{8\pi^2 c} \frac{\Gamma}{\Delta} I(\vec{r}), \quad (1)$$

where  $\Gamma$  is the spontaneous decay rate,  $I(\vec{r})$  is the intensity and  $\lambda$  is the wavelength of the  $D_2$  transition in alkali atoms [8]. The relative detuning  $\Delta$  is negative and larger than the hyperfine splitting of the excited states but smaller than the fine structure splitting. The repulsive dipole potential in mirrors for thermal atomic beams and laser-cooled atoms has been enhanced or modified employing the evanescently decaying field of SPPs propagating on gold or silver surfaces [9–13]. In all these experiments the SPPs were excited by a laser undergoing total internal reflection at a prism surface covered with a metallic film, hence in the Kretschmann configuration for SPP excitation [14]. In this arrangement, the tangential component of the wave vector of the TM (transverse magnetic) field on the dielectric prism is equal to that of the surface waves. Another possibility of momentum matching is to use a plasmonic grating coupler, as first recognized by Wood in 1902 [15]. In this case the grating vector  $2\pi m/d$  ( $m = 0, \pm 1, \pm 2, \dots$ , and  $d$  is the grating period) is added to the tangential component of the wave vector of the incident light. A simple analytical equation

---

\* Corresponding author: tomasz.kawalec@uj.edu.pl

allows for an estimate of the optimum angle of incidence  $\theta$  for a shallow grating in vacuum when the plane of incidence is perpendicular to the grating's grooves (see e.g. [16]):

$$k_0 \sqrt{\frac{\epsilon_m}{\epsilon_m + 1}} = k_0 \sin \theta \pm m \frac{2\pi}{d}, \quad (2)$$

where  $k_0$  is the free space wave vector and  $\epsilon_m$  is the real part of the relative permittivity of the metallic layer, being -22.5 for gold at 780 nm [17]. However, the exact profile of the SPPs intensity  $I(\vec{r})$  above a perfect or real grating coupler, being crucial for the dipole mirror operation (see Eq. 1), has to be computed numerically.

Using a metallic grating instead of a gold film on a prism surface in an optical atomic dipole mirror for cold atoms leads to a considerable miniaturization of the system. Complicated optical potentials may be achieved thanks to a proper preparation of metallic micro and nanostructures. Several experiments have been proposed combining subwavelength plasmonic structures with atomic and atom physics. Some of them are: modification of the probability for forbidden transitions [18], control of the spontaneous emission linewidths [19], construction of optical dipole nanolattices [20] or plasmonic waveguides [21]. In this Letter we report on the realization of a plasmonic dipole mirror for cold atoms based on a metallic grating coupler.

The heart of the experimental setup is a small ( $70 \times 22 \times 22 \text{ mm}^3$ ) rectangular ultrahigh vacuum glass cell with centrally mounted plasmonic grating coupler and a source of cold atoms above it (see Fig. 1).  $^{87}\text{Rb}$  atoms are collected in a standard background vapor loaded six beam magneto-optical trap (MOT). SPPs are excited upon illumination of the coupler by a 780 nm TM polarized laser beam of a  $730 \mu\text{m}$  type  $e^{-2}$  radius and 20-40 mW of power. The beam is blue detuned from the  $D_2 F = 2 \rightarrow F' = 3$  transition between 6 and 10 GHz and the angle of incidence is about  $14.5^\circ$ , from normal.

The optimum parameters of the grating coupler were found numerically using the rigorous coupled-wave analysis (RCWA) method [22, 23]. The SPPs intensity was optimized for a given incident beam intensity and wavelength of 780 nm corresponding to the  $D_2$  transition in rubidium atoms. For a chosen period of  $1 \mu\text{m}$  and a duty cycle of 0.5 of a gold plasmonic coupler with rectangular profile, the optimum grating depth is 35-65 nm.

The coupler consists of a 120 nm gold film supported by a 3 nm titanium adhesion layer, which was evaporated by electron beam metal deposition onto a  $7 \times 3 \text{ mm}^2$  silicon substrate. The grating structures were defined on top of the gold layer by electron beam lithography (EBL) in a 500 nm thick layer of polymethyl methacrylate (PMMA), using a scanning electron microscope (SEM). After a development step the sample was coated with a 3 nm titanium adhesive and 50 nm gold layers. The PMMA material and the residual metal layer were afterwards chemically removed in the lift off process. The EBL working area for a single grating array was lim-

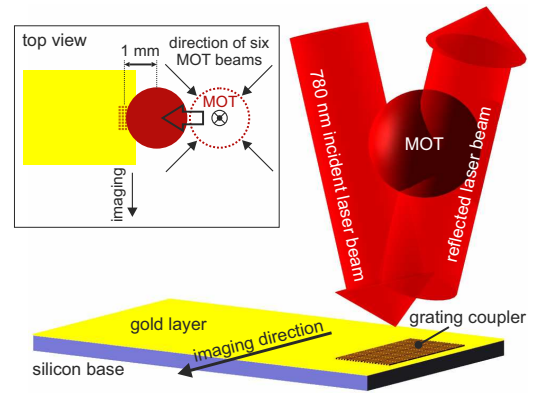


Fig. 1. Sketch of the experimental setup (not to scale). The TM polarized incident laser beam excites SPPs on a metallic grating coupler when the cloud of atoms reaches the surface. For the sake of clarity the MOT cloud is shown in its initial height only. The reflected beam is used to test the grating coupler — see Figs. 2 c) and d). Inset: top view of the setup. The horizontal arrow pointing to the left denotes shifting of the MOT cloud just before releasing it onto the dipole mirror.

ited to  $100 \times 100 \mu\text{m}^2$ . Thus, the total mirror area of  $0.4 \times 0.8 \text{ mm}^2$  was divided into 32 adjacent and identical squares arranged in a  $4 \times 8$  matrix defined as close as possible to the sample edge — see the optical microscope image in Fig. 2 a). The topography measured with atomic force microscopy (AFM) is shown in Fig. 2 b). The orientation of the ridges was chosen to be parallel to the short sample edge.

The plasmonic couplers were optically tested by measuring the zeroth order reflectivity of the TM polarized 780 nm laser beam on an auxiliary CCD camera. The SPPs presence manifests itself at a proper angle of incidence as a reduction in the reflected intensity due to the phase difference between specularly reflected and radiated light [24]. The calculated and measured angle dependent reflectivities are shown in Fig. 2 c) together with a typical CCD image of the reflected laser beam (Fig. 2 d).

The experimental sequence starts with 6.5 s of loading the magneto-optical trap followed by Doppler and molasses cooling stages. Since one of the MOT beam pairs is directed vertically, the center of the MOT and the grating coupler are initially misaligned in the horizontal plane by about 3 mm. An additional homogenous magnetic field of 1 Gauss is switched on for 6 ms during the final stages of the MOT cooling, shifting horizontally the zero of the magnetic field gradient and the atom cloud by 2 mm towards the coupler, resulting in a final misalignment of 1 mm (see inset in Fig. 1). Subsequently, the MOT beams are switched off and the cloud of about  $7 \times 10^6$  atoms and a temperature of  $40 \mu\text{K}$  is expanding and falling down under gravity. About 20 ms after switching off the MOT beams, the cloud reaches the gold grating and the laser beam exciting SPPs is switched on for 2 ms. After a time delay between 0.2 ms and 7 ms

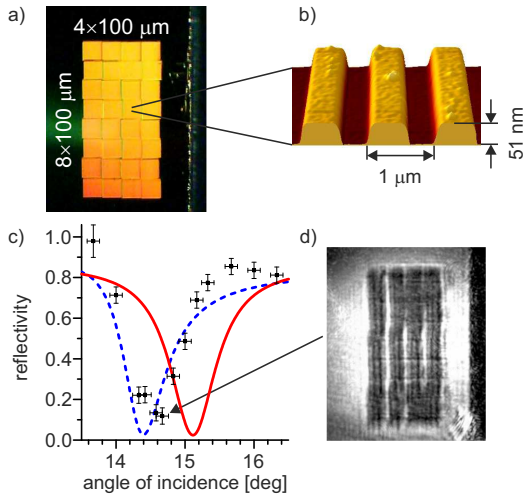


Fig. 2. Gold photon-plasmon grating coupler: a) optical microscope image under white light illumination, b) tapping mode AFM topography image of three ridges, c) angle dependent zeroth order reflectivity of the 780 nm laser beam — RCWA calculations for an ideal rectangular profile grating (solid line), modeled real grating (dashed line) and experiment (crosses). A typical CCD image of the cross section of the reflected beam is shown in d) for the optimum angle of incidence.

the reflected cloud of atoms is illuminated with the MOT beams and imaged on a cooled CCD iXon<sup>EM</sup>+ 885 camera. A typical time sequence of the reflected cloud is shown in Fig. 3. Each image requires a new experimental run and is the result of subtraction of two fluorescent photographs taken for TM and TE polarization of the incident laser beam. Since the plasmonic coupler does not work for TE polarization in our configuration, the differential images are free of the background formed by that part of the falling cloud of atoms which misses the dipole mirror. However, power fluctuations of the MOT beams used in imaging cause the outline of the silicon base to be partially visible.

In our configuration the cloud of falling atoms is much larger than the dipole mirror area. To determine the real efficiency of the plasmonic mirror we have experimentally measured the fraction of reflected atoms and compared it with the expected value based on geometric calculations. Taking into account the plasmonic mirror duration, the dimensions of the grating coupler, the initial position of the atomic cloud and its size and temperature we have found in a Monte Carlo simulation that  $0.23 \pm 0.03$  % of atoms have a chance to be reflected due to geometrical constraints. On the other hand, basing on the fluorescence imaging it was found that  $0.22 \pm 0.03$  % of the total number of falling atoms are reflected. Our plasmonic dipole mirror efficiency is thus close to 100 %. We have experimentally checked that the mirror is robust against changes in the angle of incidence in the  $\pm 0.2^\circ$  range.

The effective intensity  $I(x, y)$  of the SPPs above the

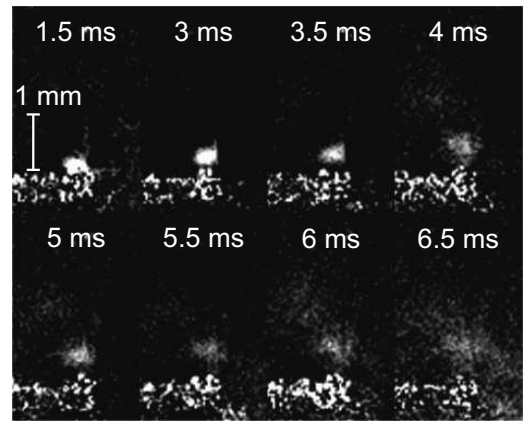


Fig. 3. Cold atomic cloud reflected off the plasmonic mirror for various times after the bounce seen along the direction shown in Fig. 1. The detuning  $\Delta$ , intensity and power of the laser beam were  $2\pi \cdot 9$  GHz,  $3.6$  W/cm<sup>2</sup> and 30 mW, respectively. The duration of the plasmonic mirror was 2 ms and the CCD integration time was 1 ms. Each image is averaged over 40 runs of the experiment.

perfect and real grating coupler was calculated using the RCWA method for optimum and suboptimum angles of laser beam incidence. The calculated optical dipole potential for <sup>87</sup>Rb atoms (see Eq. 1) above two consecutive grating ridges of a modeled real grating is shown in Fig. 4 for the same parameters as in Fig. 3. The interference of the incident and residual reflected laser beams results in a characteristic modulation of the optical dipole potential, seen in the upper half of Fig. 4. We have neglected the van der Waals atom-wall interaction in the mirror potential calculations due to the fact that it does not contribute significantly at the classical turning point distance of about 400 nm.

To calculate the dispersion of the atomic momenta induced by the reflection off the rough mirror we have numerically solved the equations of motion for atoms moving in the potential associated with SPPs. The calculation of an atom trajectory in the plasmonic potential takes place in a single sector shown in Fig. 4, i.e. in the area of  $2 \times 2$  μm<sup>2</sup>. In order to calculate the trajectory of an atom in the area of the whole grid, which is 400 μm long, the periodicity of the potential was taken advantage of. Whenever the atom reaches the left or right border of the sector, its further evolution starts from the other border with the same conditions and changed sector number. The calculation stops when the atom leaves the upper border of the sector. An exemplary trajectory of a single atom is shown by a solid white line. The velocity dispersion is obtained from the calculation for 1000 atoms with the initial velocities distribution truncated to account for initial position, temperature and size of the atom cloud. The inset of Fig. 4 shows the computed velocity dispersion of the ensemble of atoms before and after reflection, 2 μm above the grating coupler surface.

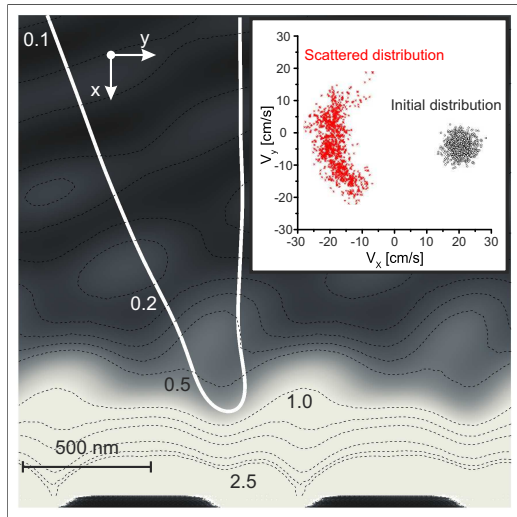


Fig. 4. Numerical simulations of the atom movement in the vicinity of a periodic plasmonic mirror. The optical dipole potential is expressed in units of  $\hbar\Gamma$ . The 2.5  $\hbar\Gamma$  equipotential line corresponds to an incident beam intensity enhancement by a factor of  $\approx 36$ . The inset shows the dispersion of the initial and final velocity in the atomic clouds just before and after the reflection.

In the present system the incident laser beam interacts directly with falling and reflected atoms during the plasmonic mirror phase via the radiation pressure force. The calculated mean number of incoherently scattered photons per atom per reflection is 5 for the same plasmonic mirror parameters as in Fig. 3. Importantly, the average photon scattering in the field of SPPs themselves is below 0.1, neglecting any atom-surface interaction.

We propose two ideas for further developing the current setup. The first one is to use the SPPs propagating on a flat gold surface outside the coupler, which means outside the excitation region (see e.g. [25]). The second one is to use a transmission grating coupler where the SPPs are excited on the opposite side of the metallic structured film than the incoming laser beam, as in the optical trap based on the micro Fresnel lens in gold [26]. As a next step towards a compact atom chip, we are planning to build a surface trap based on the plasmonic grating mirror with ultracold atoms, where sub-wavelength waveguides and focusing of SPPs are also under consideration [27].

In summary, we have demonstrated a compact optical dipole system for cold atoms and analyzed numerically individual atomic trajectories. This setup forms a basis for optical or hybrid opto-magnetic atom chips.

Financial support by the Polish Ministry of Science and Higher Education (grant no N N202 124536) is gratefully acknowledged. Part of the equipment and chemicals were financed by the European Regional Development Fund (POIG.02.02.00-00-003/08 contract) and Danish Council for Independent Research (FTP project ANAP, Contract No. 09-072949). We are grate-

ful to Tomasz Roszczynialski for assistance with the experiment and the ColdQuanta company for the UHV glass cell.

## References

- [1] A. V. Zayats, I. I. Smolyaninov, and A. A. Maradudin, *Phys. Rep.* **408**, 131 (2005).
- [2] J. Zhang, L. Zhang, and W. Xu, *J. Phys. D: Appl. Phys.* **45**, 113001 (2012).
- [3] M. A. Kasevich, D. S. Weiss, and S. Chu, *Opt. Lett.* **15**, 607 (1990).
- [4] D. Rychtarik, B. Engeser, H.-C. Nägerl, and R. Grimm, *Phys. Rev. Lett.* **92**, 173003 (2004).
- [5] H. Bender, P. W. Courteille, C. Zimmermann, and S. Slama, *Appl. Phys. B* **96**, 275 (2009).
- [6] D. Bartoszek, J. Fiutowski, T. Dohnalik, and T. Kawalec, *Optica Applicata* **40**, 535 (2010).
- [7] W. Seifert, R. Kaiser, A. Aspect, and J. Mlynek, *Opt. Commun.* **111**, 566576 (1994).
- [8] R. Grimm, M. Weidemüller, and Y. B. Ovchinnikov, *Adv. At. Mol. Opt. Phys.* **42**, 95 (2000).
- [9] T. Esslinger, M. Weidemüller, A. Hemmerich, and T. W. Hänsch, *Opt. Lett.* **18**, 450 (1992).
- [10] S. Feron, J. Reinhardt, S. L. Boiteux, O. Gorceix, J. Baudon, M. Ducloy, J. Robert, C. Miniatura, S. N. Chormaic, H. Haberland, and V. Lorent, *Opt. Commun.* **102**, 83 (1993).
- [11] H. Gauck, M. Hartl, D. Schneble, H. Schnitzler, T. Pfau, and J. Mlynek, *Phys. Rev. Lett.* **81**, 5298 (1998).
- [12] D. Schneble, M. Hasuo, T. Anker, T. Pfau, and J. Mlynek, *Rev. Sci. Instrum.* **74**, 2685 (2003).
- [13] C. Stehle, H. Bender, C. Zimmermann, D. Kern, M. Fleischer, and S. Slama, *Nature Photonics* **5**, 494 (2011).
- [14] E. Kretschmann, *Z. Phys.* **241**, 313 (1971).
- [15] R. W. Wood, *Phys. Rev.* **48**, 928 (1935).
- [16] D. Sarid and W. Challener, *Modern Introduction to Surface Plasmons — Theory, Mathematica Modeling, and Applications* (Cambridge University Press, 2010).
- [17] P. B. Johnson and R. W. Christy, *Phys. Rev. B* **6**, 4370 (1972).
- [18] A. M. Kern and O. J. F. Martin, *Phys. Rev. A* **85**, 022501 (2012).
- [19] Y. Gu, L. Wang, P. Ren, J. Zhang, T. Zhang, O. J. F. Martin, and Q. Gong, *Nano Lett.* **12**, 2488 (2012).
- [20] M. Gullans, T. G. Tiecke, D. E. Chang, J. Feist, J. D. Thompson, J. I. Cirac, P. Zoller, and M. D. Lukin, *Phys. Rev. Lett.* **109**, 235309 (2012).
- [21] W. Zheng-Ling, T. Wei-Min, Z. Ming, and G. Chuan-Yul, *Chin. Phys. B* **22**, 073701 (2013).
- [22] P. Kwiecien, “rcwa-1d,” <http://sourceforge.net/projects/rcwa-1d/> (2011).
- [23] M. G. Moharam, E. B. Grann, D. A. Pommet, and T. K. Gaylord, *J. Opt. Soc. Am. A* **12**, 1068 (1995).
- [24] H. Raether, *Surface Plasmons on Smooth and Rough Surfaces and on Gratings*, Vol. 111 (Springer-Verlag, 1988).
- [25] S. T. Koev, A. Agrawal, and V. A. A. Henri J. Lezec, *Plasmonics* **7**, 269 (2011).
- [26] O. Alloschery, R. Mathevet, and J. Weiner, *Opt. Expr.* **14**, 12568 (2006).
- [27] D. K. Gramotnev and S. I. Bozhevolnyi, *Nature Photonics* **4**, 83 (2010).

## References

- [1] A. V. Zayats, I. I. Smolyaninov, and A. A. Maradudin, “Nano-optics of surface plasmon polaritons,” *Phys. Rep.* **408**, 131 (2005).
- [2] J. Zhang, L. Zhang, and W. Xu, “Surface plasmon polaritons: physics and applications,” *J. Phys. D: Appl. Phys.* **45**, 113001 (2012).
- [3] M. A. Kasevich, D. S. Weiss, and S. Chu, “Normal-incidence reflection of slow atoms from an optical evanescent wave,” *Opt. Lett.* **15**, 607 (1990).
- [4] D. Rychtarik, B. Engeser, H.-C. Nägerl, and R. Grimm, “Two-dimensional bose-einstein condensate in an optical surface trap,” *Phys. Rev. Lett.* **92**, 173003 (2004).
- [5] H. Bender, P. W. Courteille, C. Zimmermann, and S. Slama, “Towards surface quantum optics with bose-einstein condensates in evanescent waves,” *Appl. Phys. B* **96**, 275 (2009).
- [6] D. Bartoszek, J. Fiutowski, T. Dohnalik, and T. Kawalec, “Optical surface devices for atomic and atom physics,” *Optica Applicata* **40**, 535 (2010).
- [7] W. Seifert, R. Kaiser, A. Aspect, and J. Mlynek, “Reflection of atoms from a dielectric wave guide,” *Opt. Commun.* **111**, 566576 (1994).
- [8] R. Grimm, M. Weidemüller, and Y. B. Ovchinnikov, “Optical dipole traps for neutral atoms,” *Adv. At. Mol. Opt. Phys.* **42**, 95 (2000).
- [9] T. Esslinger, M. Weidemüller, A. Hemmerich, and T. W. Hänsch, “Surface-plasmon mirror for atoms,” *Opt. Lett.* **18**, 450 (1992).
- [10] S. Feron, J. Reinhardt, S. L. Boiteux, O. Gorceix, J. Baudon, M. Ducloy, J. Robert, C. Miniatura, S. N. Chormaic, H. Haberland, and V. Lorent, “Reflection of metastable neon atoms by a surface plasmon wave,” *Opt. Commun.* **102**, 83 (1993).
- [11] H. Gauck, M. Hartl, D. Schneble, H. Schnitzler, T. Pfau, and J. Mlynek, “Quasi-2d gas of laser cooled atoms in a planar matter waveguide,” *Phys. Rev. Lett.* **81**, 5298 (1998).
- [12] D. Schneble, M. Hasuo, T. Anker, T. Pfau, and J. Mlynek, “Detection of cold metastable atoms at a surface,” *Rev. Sci. Instrum.* **74**, 2685 (2003).
- [13] C. Stehle, H. Bender, C. Zimmermann, D. Kern, M. Fleischer, and S. Slama, “Plasmonically tailored micro-potentials for ultracold atoms,” *Nature Photonics* **5**, 494 (2011).
- [14] E. Kretschmann, “The determination of the optical constants of metals by excitation of surface plasmons,” *Z. Phys.* **241**, 313 (1971).
- [15] R. W. Wood, “Anomalous diffraction gratings,” *Phys. Rev.* **48**, 928 (1935).
- [16] D. Sarid and W. Challener, *Modern Introduction to Surface Plasmons — Theory, Mathematica Modeling, and Applications* (Cambridge University Press, 2010).
- [17] P. B. Johnson and R. W. Christy, “Optical constants of the noble metals,” *Phys. Rev. B* **6**, 4370 (1972).
- [18] A. M. Kern and O. J. F. Martin, “Strong enhancement of forbidden atomic transitions using plasmonic nanostructures,” *Phys. Rev. A* **85**, 022501 (2012).
- [19] Y. Gu, L. Wang, P. Ren, J. Zhang, T. Zhang, O. J. F. Martin, and Q. Gong, “Surface-plasmon-induced modification on the spontaneous emission spectrum via subwavelength-confined anisotropic purcell factor,” *Nano Lett.* **12**, 2488 (2012).
- [20] M. Gullans, T. G. Tiecke, D. E. Chang, J. Feist, J. D. Thompson, J. I. Cirac, P. Zoller, and M. D. Lukin, “Nanoplasmonic lattices for ultracold atoms,” *Phys. Rev. Lett.* **109**, 235309 (2012).
- [21] W. Zheng-Ling, T. Wei-Min, Z. Ming, and G. Chuan-Yul, “Nanoscale guiding for cold atoms based on surface plasmons along the tips of metallic wedges,” *Chin. Phys. B* **22**, 073701 (2013).
- [22] P. Kwiecien, “rcwa-1d,” <http://sourceforge.net/projects/rcwa-1d/> (2011).
- [23] M. G. Moharam, E. B. Grann, D. A. Pommet, and T. K. Gaylord, “Formulation for stable and efficient implementation of the rigorous coupled-wave analysis of binary gratings,” *J. Opt. Soc. Am. A* **12**, 1068 (1995).
- [24] H. Raether, *Surface Plasmons on Smooth and Rough Surfaces and on Gratings*, Vol. 111 (Springer-Verlag, 1988).
- [25] S. T. Koev, A. Agrawal, and V. A. A. Henri J. Lezec, “An efficient large-area grating coupler for surface plasmon polaritons,” *Plasmonics* **7**, 269 (2011).
- [26] O. Alloschery, R. Mathevet, and J. Weiner, “All-optical atom surface traps implemented with one-dimensional planar diffractive microstructures,” *Opt. Expr.* **14**, 12568 (2006).
- [27] D. K. Gramotnev and S. I. Bozhevolnyi, “Plasmonics beyond the diffraction limit,” *Nature Photonics* **4**, 83 (2010).